

Akt Phosphorylates MstI and Prevents Its Proteolytic Activation, Blocking FOXO3 Phosphorylation and Nuclear Translocation*

Received for publication, June 1, 2007, and in revised form, August 10, 2007. Published, JBC Papers in Press, August 28, 2007, DOI 10.1074/jbc.M704542200

Sung-Wuk Jang[‡], Seung-Ju Yang[‡], Shanthi Srinivasan[§], and Keqiang Ye^{‡1}

From the Departments of [‡]Pathology and Laboratory Medicine and [§]Medicine, Division of Digestive Diseases, Emory University School of Medicine, Atlanta, Georgia 30322

Oxidative stress can induce apoptosis through activation of MstI, subsequent phosphorylation of FOXO and nuclear translocation. MstI is a common component of apoptosis initiated by various stresses. MstI kinase activation requires autophosphorylation and proteolytic degradation by caspases. The role of Akt in regulating MstI activity has not been previously examined. Here, we show that MstI is a physiological substrate of Akt. Akt phosphorylation of MstI diminishes its apoptotic cleavage by caspases and prevents its kinase activity on FOXO3. MstI directly binds to Akt, which is regulated Akt kinase activity. Akt phosphorylates MstI on the Thr³⁸⁷ residue and protects MstI from apoptotic cleavage *in vitro* and in apoptotic cells. Interestingly, Akt phosphorylation of MstI strongly inhibits its kinase activity on FOXO3. The phosphorylation mimetic mutant MstI T387E blocks H₂O₂-triggered FOXO3 nuclear translocation and apoptosis. Thus, our findings support that Akt blocks MstI-triggered FOXO3 nuclear translocation by phosphorylating MstI, promoting cell survival.

FOXO² (forkhead box O; forkhead members of the O class) are transcription factors. FOXO factors mediate cell death by regulating numerous apoptotic genes transcription (1–3). FOXO factors are insulin-sensitive transcription factors with a variety of downstream targets and interacting partners. Insulin-mediated inhibition of FOXO factors is predominantly regulated through a shuttling mechanism that distributes FOXO localization to the cytoplasm, thereby terminating its transcriptional function (4). FOXO factors contain three highly conserved putative Akt recognition motifs (RXXR(S/T), where X denotes any residue), two at the N and C termini, respectively, and one located in the forkhead domain. All FOXO proteins require Akt phosphorylation in the N terminus and in the forkhead domain to translocate from the nucleus to the cytoplasm (5). The two phosphorylated residues are essential components

for translocation, as they influence the NLS (nuclear localization sequence) function and the association with 14-3-3 proteins (2). Recently, Bonni and co-workers demonstrated that MstI mediates oxidative stress-induced neuronal apoptosis through FOXO factors by phosphorylating FOXO3 on Ser²⁰⁷. This phosphorylation triggers its nuclear translocation and disrupting the association between 14-3-3 and FOXO in the cytoplasm (6).

MstI belongs to class II GC (protein Ser/Thr) kinase (7), which contains 487 residues and predominantly resides in the cytoplasm. MstI consists of an N-terminal catalytic domain in the Ste20 class, followed by a non-catalytic tail comprising of an autoinhibitory domain and a coiled-coil domain that mediates dimerization (8). It has been suggested that, physiologically, MstI exists as an autoinhibitory homodimer that is activated after post-translational modification such as phosphorylation and/or cleavage. Although caspase-mediated cleavage removes the C-terminal regulatory domain, which is associated with an increase in MstI activity, there is evidence that caspase-mediated cleavage alone cannot activate MstI and both phosphorylation and proteolysis are necessary to activate fully this enzyme (9–11). Indeed, Lee *et al.* (12) purified a 34-kDa protein that was identified as MstI/MstII but did not have kinase activity. Several phosphorylation sites have now been identified in MstI, namely Thr¹⁷⁵, Thr¹⁷⁷, Thr¹⁸³, Thr¹⁸⁷, Ser³²⁷, and Thr³⁸⁷ (9, 11). Of these, Thr¹⁸³ and Thr¹⁸⁷ appear to be essential for kinase activity (11). It has been proposed before that phosphorylation of MstI on Thr¹⁸³ and possibly Thr¹⁸⁷ is induced by an existing active MstI (11). Overexpression of MstI alone is sufficient to initiate apoptosis in various cells, which involves activation of SAPK (stress-activated protein kinase)/JNK (13), p53 (14), FOXO (6). MstI cycles rapidly and continuously through the nucleus (6, 15), and associates with DAP-4 (death-associated protein-4) in the nucleus (14), where the catalytic fragment generated during apoptosis triggers chromatin condensation (15, 16). MstI potentially interacts with both growth inhibitory proteins RASSF1A and NORE1A. Overexpression of RASSF1A increases kinase activity of MstI in intact cells (17), and facilitates MstI activation and thereby promotes apoptosis induced by death receptor signaling (18). Interestingly, PP2A treatment up-regulates MstI kinase activity, whereas EGF treatment decreases its kinase activity, suggesting that phosphorylation on the resting MstI negatively modulates its kinase activity. Mitogenic signal might trigger its further phosphorylation, resulting in reduction of its kinase activity (7).

* This work was supported by grants from the National Institutes of Health (R01, NS045627) (to K.Y.). The costs of publication of this article were defrayed in part by the payment of page charges. This article must therefore be hereby marked "advertisement" in accordance with 18 U.S.C. Section 1734 solely to indicate this fact.

¹ To whom correspondence should be addressed: Dept. of Pathology and Laboratory Medicine, Emory University School of Medicine, Atlanta, GA 30322. Tel.: 404-712-2814; E-mail: kye@emory.edu.

² The abbreviations used are: FOXO, forkhead box O; MstI, mammalian Sterile20-like 1; GST, glutathione S-transferase; HRP, horseradish peroxidase; DAPI, 4',6-diamidino-2-phenylindole.

In this study, we demonstrate that Akt binds and phosphorylates MstI, leading to its resistance against apoptotic cleavage and inhibition of its kinase activity on FOXO3. In addition, we show that MstI T387E, an Akt phosphorylation mimetic mutant, blocks FOXO3 nuclear translocation regardless of H₂O₂ stimulation, preventing apoptosis. In contrast, MstI T387A, a nonphosphorylated mutant, strongly phosphorylates FOXO3 and triggers its nuclear translocation, enhancing cell death.

EXPERIMENTAL PROCEDURES

Cells and Reagents—HEK293 cells were maintained in medium A (DMEM with 10% fetal bovine serum and 100 units of penicillin-streptomycin) at 37 °C with 5% CO₂ atmosphere in a humidified incubator. EGF was from Roche Applied Sciences. Anti-caspase-3 and anti-tubulin antibodies were from Santa Cruz Biotechnology, Inc. Anti-Myc, anti-phospho-Akt-473, and anti-Akt were from Cell Signaling. Anti-MstI and anti-phospho-MstI antibodies and active Akt protein were from Upstate Biotechnology, Inc. Anti-Foxo3 Ser²⁰⁷ antibody was from Invitrogen. All the chemicals not included above were from Sigma.

Cell-free Apoptotic Solution Preparation and MstI Cleavage Assay—The procedures are exactly as described (19). Briefly, the pellets of 293 cells were washed once with ice-cold phosphate-buffered saline and resuspended in 5 vol of buffer A, supplemented with protease inhibitors. After sitting on ice for 15 min, the cells were broken by passing 15 times through a G22 needle. After centrifugation in a microcentrifuge for 5 min at 4 °C, the supernatants were further centrifuged at $10^5 \times g$ for 30 min in an ultracentrifuge (Beckman). The resulting supernatants were used for *in vitro* apoptosis assay. The purified activated caspase 3 was added into S-100 extract to initiate caspase cascade. After 1 h of incubation at 37 °C, *in vitro* transcribed and translated MstI protein, which was treated with or without active Akt, or purified GST-MstI recombinant proteins were introduced and incubated for another hour. The reaction mixture was analyzed by immunoblotting with anti-GST-HRP or autoradiography, respectively.

In Vitro Binding Assays—GST fusion proteins were prepared and coupled to glutathione-Sepharose beads. HEK293 cells were transfected with HA-tagged Akt constructs, and the cells were washed once in phosphate-buffered saline, and lysed in 1 ml of lysis buffer A (50 mM Tris, pH 7.4, 40 mM NaCl, 1 mM EDTA, 0.5% Triton X-100, 1.5 mM Na₃VO₄, 50 mM NaF, 10 mM sodium pyrophosphate, 10 mM sodium β -glycerophosphate, 1 mM phenylmethylsulfonyl fluoride, 5 mg/ml aprotinin, 1 mg/ml leupeptin, 1 mg/ml pepstatin A), and centrifuged for 10 min at $14,000 \times g$ at 4 °C. The cell lysates were incubated with GST protein-conjugated glutathione beads at 4 °C for 3 h. After incubation, the beads were washed three times with 500 μ l of lysis buffer each time. The agarose then was resuspended in 30 μ l of sample buffer separated by SDS-PAGE followed by immunoblotting analysis.

Cytochemical Staining of Apoptotic Cells—MstI-transfected cells were treated with or without 35 μ M etoposide for 16 h, followed by incubation with a fluorescent dye MR(DEVD)2 for 1 h. The red cells are considered apoptotic. Morphological

changes in the nuclear chromatin of cells undergoing apoptosis were detected by staining with 4,6-diamidino-2-phenylindole (DAPI) as described (20). Totally, about 500 nuclei were counted under different fields. The Picture was taken on an Olympus IX71 invert fluorescent microscope.

In Vitro Kinase Assay—Ectopically expressed MstI were immunoprecipitated with glutathione beads. After extensive washing, the complex was employed in a kinase assay. The precipitated MstI were incubated with 2 μ g of histone H2B or FOXO3 in 20 μ l of kinase reaction buffer (20 mM Tris, pH 7.5 with 10 mM MgCl₂) containing 25 μ M ATP and 2.5 μ Ci of [γ -³²P]ATP for 20 min at 30 °C. Reactions were terminated by adding 7 μ l of Laemmli's sample buffer and boiling for 5 min. A portion of the sample (15 μ l) was separated on a SDS-polyacrylamide gel and autoradiographed or analyzed by PhosphorImage analyzer.

Caspase-3 Activity Assay—Caspase-3 activity was measured by means of the CasPACE Assay System Fluorometric kit (Promega Corp., Madison, WI). Cells were initially seeded at a density of 1×10^6 in 10-cm dishes, and transfected with various GST-tagged MstI constructs, followed by 35 μ M VP16 treatment for 24 h, caspase-3 activity was measured by the cleavage of the fluorometric substrate Ac-DEVD-AMC according to the manufacturer's instructions.

Subcellular Fractionation—Briefly, GST-MstI constructs transfected HEK293 cells (1×10^6 to 5×10^6 /ml) were washed once with 1 ml of phosphate-buffered saline and once with 1 ml of lysis buffer (10 mM Hepes, 10 mM KCl, 1.5 mM MgCl₂, 0.5 mM phenylmethylsulfonyl fluoride, 10 μ g/ml leupeptin, pH 7.9). Cells were lysed by suspending the cell pellet in 20 μ l of lysis buffer containing 0.1% Nonidet P-40 for 10 min on ice. To isolate nuclei, the lysates were microcentrifuged for 5 min at $12,000 \times g$, and the nuclear pellet was washed with lysis buffer without Nonidet P-40. Nuclear proteins were obtained by resuspending the nuclear pellet in 20 μ l of extraction buffer (420 mM NaCl, 20 mM Hepes, 1.5 mM MgCl₂, 0.2 mM EDTA, 25% glycerol, pH 7.9) for 10 min at 4 °C. The nuclear suspension was microcentrifuged, the pellet was discarded, and the supernatant was diluted in dilution buffer (50 mM KCl, 20 mM Hepes, 0.2 mM EDTA, 20% glycerol, pH 7.9).

RESULTS

Akt Phosphorylates MstI on Thr³⁸⁷—In exploring the sequence of MstI, we noticed that amino acids 120, RLRNKTL; 345, TVRVAST; 387, KRRDET^M, correspond to a motif that is identified as a consensus Akt phosphorylation element present in numerous Akt substrates (Fig. 1A). We prepared GST-recombinant proteins from three fragments of MstI containing putative phosphorylation domains, and examined the ability to be phosphorylated by Akt through *in vitro* kinase assays. Fragment (amino acids 300–487) and positive control GSK- β were robustly phosphorylated by active Akt, as manifested by immunoblotting analysis with anti-phospho-Akt substrate antibody, which recognizes the consensus Akt phosphorylation elements R/KXR/KXX(S/T) present in numerous Akt substrates. By contrast, fragments 1–100 and 1–160 and GST alone were not phosphorylated (Fig. 1B, left panel). Similar results were also observed in the presence of [γ -³²P]ATP (data not shown).

Akt Phosphorylates Mst1, Inhibiting Its Apoptotic Activity

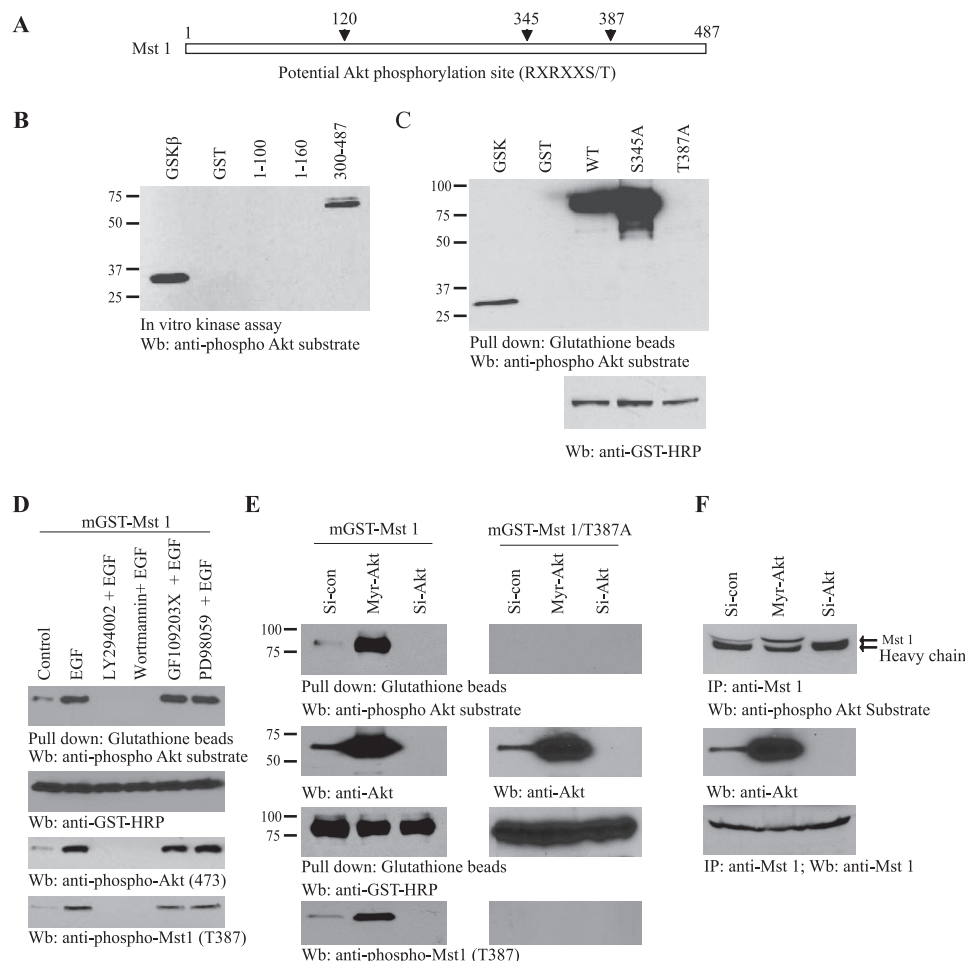


FIGURE 1. Akt phosphorylates Mst1 on Thr³⁸⁷. A, diagram of human Mst1. Mst1 possesses three putative Akt phosphorylation motifs (RXXXS/T) as indicated (▼) with residue numbers. B, *in vitro* Akt kinase assay. Purified recombinant GST-fusion proteins were incubated with active Akt at 30 °C for 30 min. Fragments 300–487 and positive control GSK-β were robustly phosphorylated, while fragments 1–100 and 1–160 were not. C, Thr³⁸⁷ residue in Mst1 is phosphorylated by Akt. GST-Mst1 wild-type, S345A and T387A and GST alone were incubated with active Akt at 30 °C for 30 min and monitored by immunoblotting with anti-phospho-Akt substrate antibody. Wild-type Mst1 and S345A but not T387A mutant were strongly phosphorylated. GSK-β was employed as a positive control (*upper panel*). Equal amounts of GST proteins were employed (*lower panel*). D, PI 3-kinase inhibitor blocks Mst1 phosphorylation on Thr³⁸⁷. GST-Mst1 was transfected into HEK293 cells, followed by 10 μM LY294002 or GF109203X pretreatment. The cells were then treated with EGF for 10 min. EGF stimulated Mst1 phosphorylation, which was diminished by PI 3-kinase but not PKC inhibitor pretreatment (*top panel*). Expression of GST-Mst1 and Akt phosphorylation were verified (*2nd and 3rd panels*). Immunoblotting with anti-phospho-Mst1 T387 antibody confirmed phospho-Akt substrate antibody results (*bottom panel*). E, Akt is required for Mst1 phosphorylation. GST-Mst1 wild-type and T387A were transfected into HEK293 cells. The transfected cells were infected with adenovirus expressing active Myristoylated Akt or shRNA of Akt1. Active Akt provoked strong phosphorylation in wild-type Mst1 and depletion of Akt abolished Mst1 phosphorylation (*top left panel*). No phosphorylation was detected on Mst1 T387A mutant (*top right panel*). Verification of Akt and GST-Mst1 expression (*2nd and 3rd panels*). Immunoblotting with anti-phospho-Mst1 Thr³⁸⁷ antibody confirmed phospho-Akt substrate antibody's results (*bottom panel*). F, active Akt robustly phosphorylates endogenous Mst1 and knocking down of Akt eliminates its phosphorylation.

Mutation with T387A but not S345A abolished Mst1 phosphorylation by active Akt, suggesting that the Thr³⁸⁷ residue can be phosphorylated by Akt *in vitro* (Fig. 1C, *upper panel*), fitting with previous report that Thr³⁸⁷ is a phosphorylation site on Mst1 (11). To explore whether Mst1 can be phosphorylated by Akt in intact cells, we transfected HEK293 cells with GST-tagged Mst1 and pretreated the cells with various inhibitors, followed by EGF stimulation. The transfected GST proteins were pulled down with glutathione beads and monitored by immunoblotting analysis with anti-phospho-Akt substrate antibody. EGF treatment triggered a potent phosphorylation

in Mst1, which was substantially decreased by PI 3-kinase inhibitor LY294002 and Wortmannin but not PKC inhibitor GF109203X or MEK1 inhibitor PD98059 (Fig. 1D, *top panel*). Equal amounts of GST fusion proteins were precipitated (Fig. 1D, *2nd panel*). Akt phosphorylation status tightly coupled to Mst1 phosphorylation (*3rd panel*). Immunoblotting with anti-phospho-Mst1 Thr³⁸⁷ antibody further confirmed that Akt phosphorylates Mst1 on Thr³⁸⁷ residue in intact cells (Fig. 1D, *bottom panel*). To ascertain that Mst1 is the physiological substrate of Akt, we transfected HEK293 cells with GST-Mst1, and infected the transfected cells with adenovirus expressing plasma membrane localized active myristoylated Akt or sh-RNA of Akt. Mst1 was pulled down with glutathione beads. Immunoblotting analysis reveals that Mst1 was robustly phosphorylated by Myr-Akt, and its phosphorylation was completely blocked when Akt was depleted (Fig. 1E, *top left panel*). Mutation of Thr³⁸⁷ into alanine totally abolished Mst1 phosphorylation by membrane-localized active Akt (Fig. 1E, *top right panel*). Immunoblotting with anti-phospho-Mst1 Thr³⁸⁷ antibody verified these observations (Fig. 1E, *bottom panels*). Endogenous Mst1 exhibited the similar results (Fig. 1F). Thus, Akt phosphorylates Mst1 *in vitro* and *in vivo*.

Akt Associates with Mst1—Akt can exist in a stable complex with several of its substrate proteins (e.g. Mdm2, TSC2, EDG-1) and can also interact with many proteins that do not serve as Akt substrate, but rather seem to play a modulatory role in Akt regulation (21). To

explore whether Mst1 binds to Akt, we transfected HA-Akt into HEK293 cells with GST-Mst1 construct, and pretreated the transfected cells with various pharmacological agents, followed by EGF for 10 min. GST-Mst1 proteins was pulled down with glutathione beads, and the associated proteins were analyzed with anti-HA antibody. Mst1 potently associated with Akt, and EGF treatment enhanced their binding. PI3-kinase inhibitor wortmannin or LY294002 pretreatment markedly attenuated the association. By contrast, PKC inhibitor GF109203X had no effect (Fig. 2A, *top panel*). Equal amounts of transfected GST-Mst1 and HA-Akt proteins and Akt phosphorylation status

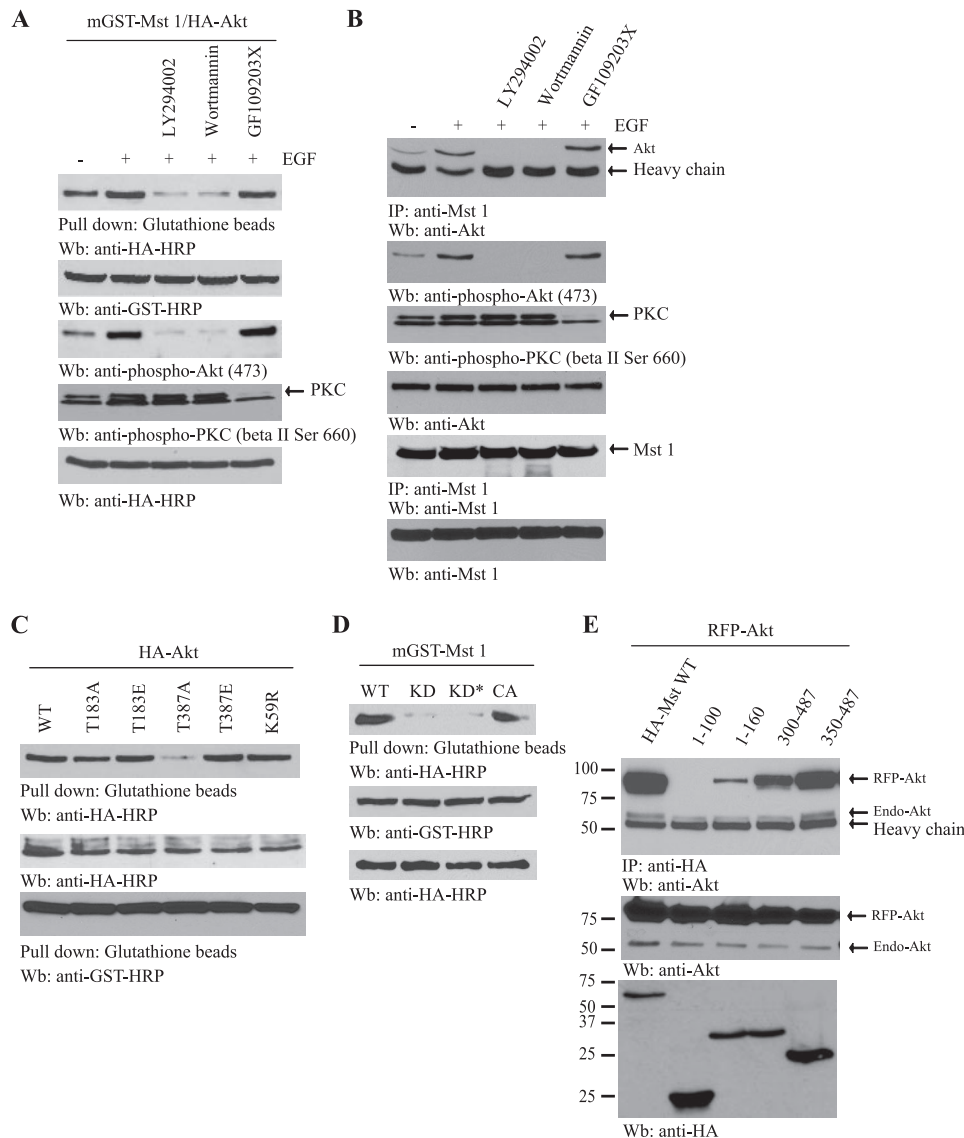


FIGURE 2. Akt associates with Mst1. A, PI 3-kinase signaling regulates Mst1/Akt interaction. GST-Mst1 and HA-Akt were cotransfected into HEK293 cells, followed by various pharmacological agents pretreatment for 30 min. EGF was introduced into the transfected cells for another 10 min. EGF enhanced the association and PI 3-kinase inhibitors but not PKC inhibitor pretreatment abolished the interaction between Mst1 and Akt (*top panel*). The expression of transfected proteins was verified (*2nd and bottom panels*). Confirmation of Akt phosphorylation status (*3rd panel*). Verification of the inhibitory effect by PKC inhibitor GF109203X (*4th panel*). B, PI 3-kinase signaling regulates the association between endogenous Mst1 and Akt. Verification of the inhibitory effect by PKC inhibitor GF109203X (*3rd panel*). Equal amounts of Mst1 was pulled-down (*5th panel*). C, Thr³⁸⁷ phosphorylation is essential for Mst1 binding to Akt. HA-Akt was cotransfected into HEK293 cells with various GST-Mst1 constructs. GST pull-down assay demonstrates that T387A failed to associate with Akt (*top panel*). Verification of transfected proteins (*middle and bottom panels*). D, Akt kinase activity is required for its association with Mst1. GST-Mst1 and various Akt constructs were cotransfected into HEK293 cells. GST pull-down demonstrates that KD or phosphorylation mimetic Akt-KD* failed to bind Mst1. By contrast, Akt-wild-type and constitutively active Akt-CA strongly bound to Mst1 (*top panel*). Similar expression level of transfected proteins was verified (*middle and bottom panels*). E, *in vitro* binding mapping assay. A variety of HA-Mst1 fragments and RFP-Akt were cotransfected into HEK293 cells. Immunoprecipitation assay reveals that the C terminus of Mst1 is involved in binding Akt (*top panel*). Verification of transfected proteins (*middle and bottom panels*).

were verified (Fig. 2A, *2nd, 3rd, and bottom panels*). As control, PKC kinase inhibitory effect by GF109203X was verified (Fig. 2A, *4th panel*).

To determine whether endogenous Mst1 binds to Akt in HEK293 cells, we conducted coimmunoprecipitation with anti-Akt antibody. Compared with control cells, EGF treatment stimulated robust interaction between Mst1 and Akt. PI3-kinase inhibitors pretreatment significantly decreased the bind-

ing; by contrast, PKC inhibitor exhibited negligible effect (Fig. 2B, *top panel*). Akt phosphorylation was robustly blocked by PI 3-kinase inhibitors (Fig. 2B, *2nd panel*). As the control, PKC kinase inhibitory effect by GF109203X was verified (Fig. 2B, *3rd panel*). Similar levels of total protein lysate were employed in all samples, and equal amounts of Mst1 was pulled-down (Fig. 2B, *4th, 5th, and bottom panels*). Thus, activation of PI 3-kinase pathway is indispensable for the interaction between Akt and Mst1. To further explore the interaction between Akt and Mst1, we transfected HA-Akt into HEK293 cells with various GST-tagged Mst1 constructs. GST pull-down assay demonstrates that Akt robustly interacted with various Mst1 proteins except T387A, a mutant unable to be phosphorylated by Akt (Fig. 2C). These results suggest that Mst1 phosphorylation by Akt is essential for its association with Akt. Nevertheless, Mst1 phosphorylation on Thr¹⁸³ or its kinase activity is not required for its interaction with Akt. To explore whether Akt kinase activity is also implicated in this event, we conducted coimmunoprecipitation studies with a variety of Akt constructs. Mst1 strongly bound to both wild-type and constitutively active Akt-CA (T308DS473D), but it failed to interact with kinase-dead Akt-KD (K179M) or phosphorylation mimetic Akt lacking kinase activity Akt-KD* (T308DS473DK179M) (Fig. 2D). These results indicate that Akt phosphorylation status is not imperative for its association with Mst1; instead, its kinase activity is critical for this event. Mapping assay with a variety of Mst1 fragments reveals that the C terminus of Mst1

was strongly involved in binding to Akt (Fig. 2E). Therefore, Akt interacts with Mst1, for which Akt kinase activity is indispensable.

Akt Phosphorylation of Mst1 Prevents Its Proteolytic Cleavage and Blocks Apoptosis—Mst1 undergoes several proteolytic cleavage during apoptosis (10, 13). Mst1 can be cleaved at DEMD326 and TMTD349 to generate catalytically active enzyme of 36 and 40 kDa, respectively. To examine whether Akt phosphorylation could suppress its degradation by

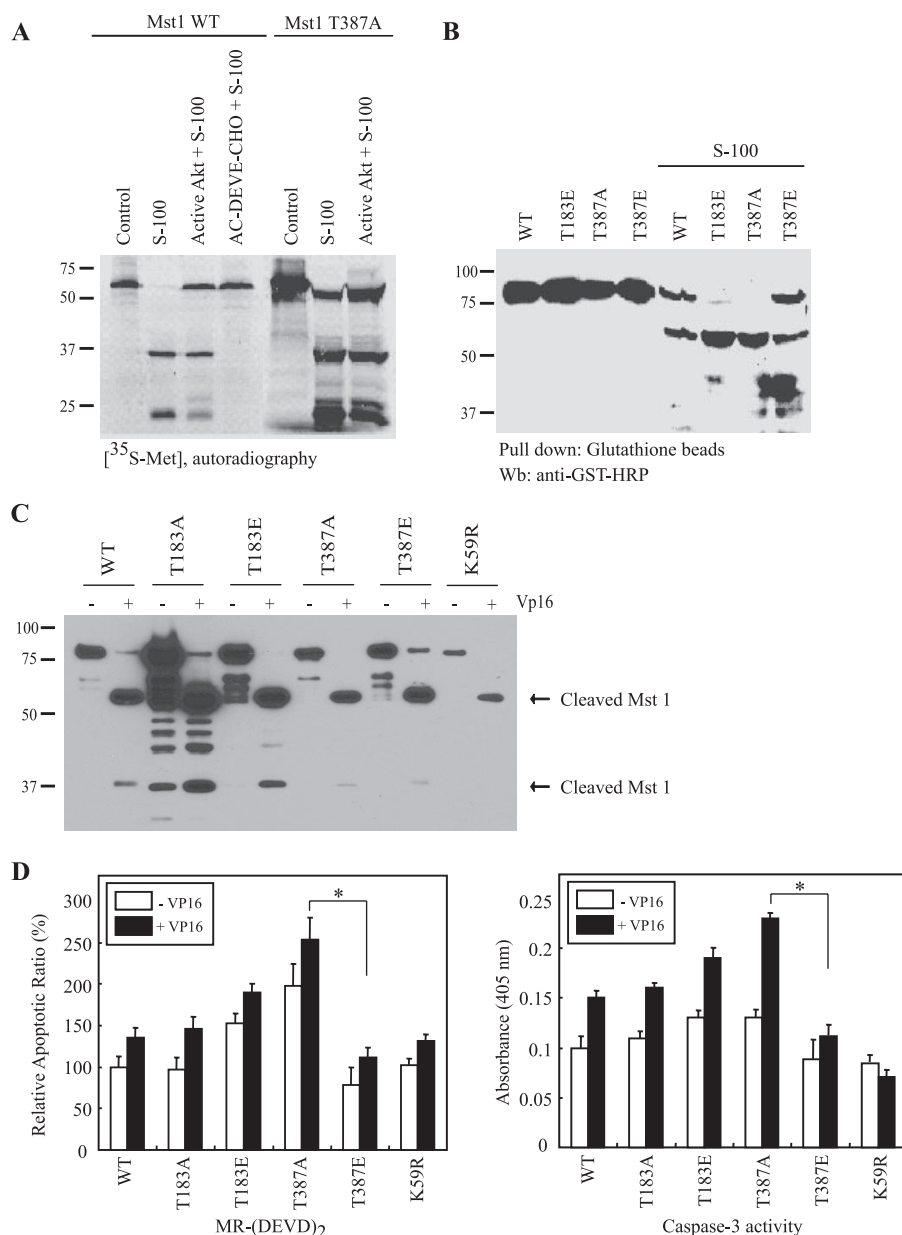


FIGURE 3. Akt phosphorylation of MstI prevents its proteolytic cleavage and blocks apoptosis. *A*, *in vitro* cleavage assay with active cell-free apoptotic solution. Wild-type and T387A MstI proteins were radiolabeled with [³⁵S]methionine from *in vitro* transcription and translation, followed by active Akt phosphorylation. The reaction mixture was subjected to apoptotic solution cleavage. Wild-type MstI was actively cleaved, but Akt phosphorylation decreased its degradation. In contrast, Akt had no effect on T387A mutant. *B*, *in vitro* cleavage assay with recombinant MstI mutant proteins. Akt phosphorylation mimetic mutant T387E resisted caspases cleavage, whereas T387A, a nonphosphorylated mutant, was completely degraded. *C*, Akt phosphorylation mimetic MstI mutant resists cleavage in apoptotic cells. Variety of MstI constructs were transfected into HEK 293 cells, followed by 35 μ M VP16 treatment for 16 h. T387E was resistant against VP16-triggered apoptotic cleavage. *D*, quantitative apoptotic assay. The cells were transfected and treated as described above. The apoptotic cells were analyzed with MR(DEVD)₂, a fluorescent turning to red upon caspase-3 cleavage (left panel). T387A MstI-transfected cells displayed the most apoptosis, whereas T387E MstI-transfected cells displayed the least apoptosis. Caspase-3 activity assay (right panel). The cell lysates from the above cells were analyzed with caspase-3 activity kit. Caspase-3 activity correlated with quantitative cell death results. Values are means (\pm S.D.) of three independent experiments. The significance of the difference between T387A and T387E groups was analyzed with the Student's *t* test (*, *p* < 0.01).

caspases, we radiolabeled wild-type and T387A mutant MstI with [³⁵S]methionine. After incubation with active Akt, the reaction mixture was introduced into active cell-free apoptotic solution, consisting of HEK293 cell cytosol supplemented with purified active caspase 3 (19). Autoradiography shows that wild-type MstI was completely cleaved in active S-100, yielding

37- and 25-kDa fragments, which was completely blocked by caspase inhibitor (Fig. 3A, lanes 2 and 4). Akt phosphorylation evidently reduced its proteolytic degradation, leading to a portion of full-length MstI remained intact. In contrast, MstI T387A mutant was actively cleaved irrespective of Akt treatment, as equal amounts of 37- and 25-kDa cleaved products presented in both samples (Fig. 3A, lanes 6 and 7), suggesting that Akt phosphorylation of MstI protects it from apoptotic degradation. The phosphorylation of MstI was verified by anti-phospho-MstI Thr³⁸⁷ antibody (data not shown). To compare whether different MstI mutants possess distinct apoptotic cleavage activities, we prepared numerous GST-MstI recombinant proteins and incubated with active cell-free apoptotic solution. Immunoblotting analysis reveals that T387A was completely degraded and T183E cleavage was faster than wild-type MstI. Nonetheless, T387E exhibited the slowest degradation rate, indicating that Akt phosphorylation protects it from caspase cleavage. These data suggest that Thr¹⁸³ phosphorylation enhances MstI apoptotic cleavage, and blockade of MstI phosphorylation by Akt evidently facilitates its apoptotic cleavage (Fig. 3B).

To investigate whether Akt phosphorylation of MstI protects it from proteolytic degradation in apoptotic cells, we transfected HEK293 cells with various MstI constructs and treated the transfected cells with VP16. Wild-type MstI and kinase-dead K59R mutant were actively cleaved upon VP16 treatment. Interestingly, T183A was evidently cut regardless of VP16 stimulation. Notably, T387E, which mimics Akt phosphorylation, somehow resisted against apoptotic cleavage compared with other constructs (Fig. 3C). Apoptotic assay with a fluorescent dye MR(DEVD)₂, which turns red upon caspase-3 cleavage, showed that transfection of T387A alone initiated the most apoptosis, followed by T183E. However, kinase-dead MstI (K59R), wild-type MstI, and T183A displayed similar apoptotic activities. The lowest apoptosis occurs to Akt phosphorylation mimetic mutant

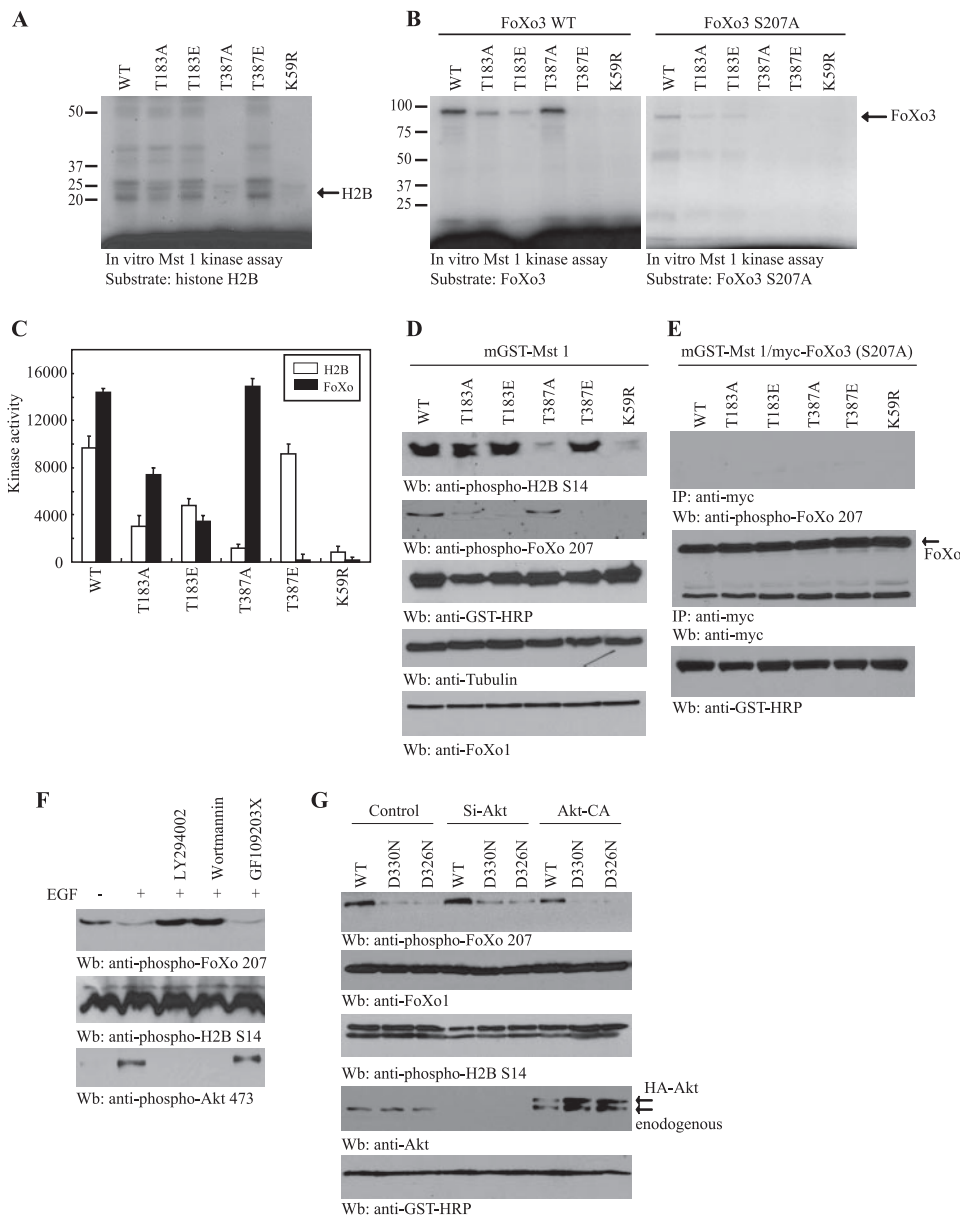


FIGURE 4. Akt phosphorylation of Mst1 inhibits its kinase activity on FOXO3. *A*, Mst1 kinase assay. *In vitro* kinase assay with histone H2B and GST-Mst1 recombinant proteins in the presence of [γ - 32 P]ATP. The radiolabeled H2B was resolved on SDS-PAGE. *B*, T387A strongly phosphorylates FOXO3. *In vitro* kinase assay with Myc-tagged FOXO3 and its mutant S207A using GST-Mst1 recombinant proteins in the presence of [γ - 32 P]-ATP. The radiolabeled FOXO3 proteins were resolved on SDS-PAGE. *C*, quantitative analysis of Mst1 kinase activity on H2B and FOXO3. After the *in vitro* kinase assay, the reaction mixture were spotted on filter paper. After extensive washing and dry, the radiolabeled substrates were counted with liquid scintillation counter. T387A and T387E Mst1 mutants displayed opposite phosphorylation activity on FOXO3. Interestingly, T387E strongly phosphorylated H2B. *D*, T387A Mst1 blocked H2BS14 phosphorylation in transfected cells, fitting with *in vitro* kinase assay results. *E*, T387A strongly provokes FOXO3 Ser²⁰⁷ phosphorylation in transfected cells. *F*, blocking Akt phosphorylation of Mst1 enhances Ser²⁰⁷ phosphorylation in FOXO3. HEK293 cells were treated with various pharmacological inhibitors. The cell lysates were analyzed by immunoblotting with various antibodies. Akt phosphorylation inversely correlated with FOXO3 Ser²⁰⁷ phosphorylation (top and bottom panel). By contrast, H2BS14 phosphorylation was not affected (middle panel). *G*, Mst1 apoptotic cleavage is required for Akt-mediated mechanism. HEK293 cells were cotransfected with GST-Mst1 wild-type or caspase cleavage-resistant constructs and active Akt-CA or siRNA. Ablation of Akt enhanced FOXO3 Ser²⁰⁷ phosphorylation, whereas overexpression of active Akt repressed FOXO3 phosphorylation (top panel). Equal amounts of samples were loaded (2nd panel). Immunoblotting of H2BS14 in transfected cells (3rd panel). Verification of Akt and transfected Mst1 (4th and bottom panels).

T387E. VP16 treatment virtually displayed the similar apoptotic activity pattern with the most apoptosis in T387A cells and the least cell death in T387E (Fig. 3D, left panel). Caspase-3 activity assay revealed the parallel effects (Fig. 3D, right panel).

Therefore, our data support that Akt phosphorylates Mst1, protects Mst1 from apoptotic degradation and suppresses the programmed cell death.

Akt Phosphorylation of Mst1 Inhibits Its Kinase Activity on FOXO3—Previous studies demonstrate that histone H2B and FOXO3 are the substrates of Mst1 (6, 16). Histone H2BS14 is reported to be directly phosphorylated by Mst1 during apoptosis to trigger chromatin condensation (16). To explore the effect of Akt phosphorylation on Mst1 kinase activity, we conducted *in vitro* kinase assay with various Mst1 recombinant proteins using H2B as a substrate. As expected, both wild-type and Mst1 T183E mutant potentially phosphorylated H2B, whereas Mst1 T183A exhibited a decreased activity. The kinase-dead Mst1 K59R failed to phosphorylate H2B. Surprisingly, Mst1 T387E, an Akt phosphorylation mimetic mutant, displayed the strongest kinase activity on H2B, while its unphosphorylated mutant T387A was unable to phosphorylate H2B (Fig. 4A). These results suggest that Akt phosphorylation of Mst1 enhances its kinase activity on H2B. However, when we performed Mst1 kinase assay with FOXO3 as a substrate, we found that Mst1 T183E exhibited a kinase activity much less than that of wild-type or T183A Mst1. Interestingly, Mst1 T387A robustly phosphorylated FOXO3. By contrast, both Mst1 K59R and T387E failed to phosphorylate FOXO3 (Fig. 4B, left panel). Mst1 phosphorylates FOXO3 on Ser²⁰⁷ and triggers its nuclear translocation (6). To confirm the specificity of FOXO3 phosphorylation by Mst1, we conducted Mst1 kinase assay with S207A FOXO3 recombinant protein as a substrate. None of Mst1 proteins was able to phosphorylate the mutant (Fig. 4B, right panel), verifying that Ser²⁰⁷ is the Mst1 phosphorylation site and our

kinase assay for FOXO3 is specific. Quantitative analysis showed that Mst1 T387A and T387E mutants exhibited the completely opposite kinase activities on H2B and FOXO3. Interestingly, Mst1 T183A and T183E possessed inverse kinase

activities on H2B and FOXO3 as well (Fig. 4C). To further examine the effect of H2B and FOXO3 phosphorylation by various MstI mutants, we performed immunoblotting analysis with MstI-transfected cells. Compared with the pronounced kinase activities by other MstI proteins, neither MstI T387A nor MstI K59R was able to trigger H2BS14 phosphorylation in the transfected cells (Fig. 4D, *top panel*), consistent with the *in vitro* kinase assay results. Interestingly, both wild-type MstI and T387A mutant strongly phosphorylated FOXO3, whereas MstI T387E and MstI K59R mutants failed to phosphorylate FOXO3 in the transfected cells, fitting with the *in vitro* findings. Similarly, MstI T187A displayed slightly higher kinase activity on FOXO3 than MstI T183E did (Fig. 4D, *2nd panel*). As expected, we did not observe any phosphorylation on FOXO3 S207A mutant (Fig. 4E). To further confirm the notion that blocking Akt phosphorylation on MstI enhances its kinase activity on FOXO3, we treated HEK293 cells with various pharmacological inhibitors and monitored FOXO3 Ser²⁰⁷ and H2BS14 phosphorylation. EGF suppressed FOXO3 Ser²⁰⁷ phosphorylation, and inhibition of Akt activation by PI 3-kinase inhibitors lead to marked phosphorylation of FOXO3 Ser²⁰⁷. By contrast, the PKC inhibitor GF109203X had no effect. Nevertheless, H2BS14 phosphorylation was not affected by any of the above treatments (Fig. 4F). Thus, these data demonstrate that blockage of Akt activity strongly promotes MstI kinase activity on FOXO3, but it has no effect on H2B. To investigate whether MstI apoptotic cleavage is required for Akt-mediated mechanism, we employed MstI D326N and D330N mutants, which resist against proteolytic cleavage by caspases. Compared with potent Ser²⁰⁷ phosphorylation in FOXO3 by wild-type MstI, both MstI D326N and D330N mutants barely phosphorylated FOXO3. Ablation of endogenous Akt enhanced MstI kinase activity on FOXO3, which was substantially attenuated by overexpression of active Akt-CA. The apoptotic cleavage-resistant MstI mutants displayed negligible kinase activity on FOXO3 regardless of Akt (Fig. 4G, *top panel*). By contrast, H2BS14 was not obviously altered no matter which MstI construct was transfected, and Akt protein level had no significant affect either (Fig. 4G, *3rd panel*). Hence, MstI apoptotic cleavage is required for Akt to exert its regulatory effect on MstI kinase activity to FOXO3 but not to H2B.

Akt Phosphorylation Mimetic MstI T387E Prevents H₂O₂-triggered FOXO3 Nuclear Translocation—Upon oxidative stress, MstI phosphorylates FOXO3 on Ser²⁰⁷ and triggers its nuclear translocation and induces neuronal cell death (6). To explore the physiological consequence of Akt phosphorylation of MstI, we monitored FOXO3 nuclear translocation in cotransfected HEK293 cells in the presence or absence of H₂O₂ stimulation. In the absence of H₂O₂, a portion of FOXO3 (18%) resided in the nucleus when cotransfected with wild-type MstI and 74% of FOXO3 translocated into the nucleus in T183E-cotransfected cells. Interestingly, 88% of FOXO3 occurred in the nucleus when cotransfected with T387A. Negligible nuclear FOXO3 was found when cotransfected with T187A, T387E, or K59R. In response to H₂O₂ treatment, 78% FOXO3 distributed in the nucleus when cotransfected with wild-type MstI, and the ratios increased to 93 and 97% in T183E and T387A cotransfected cells. By contrast, ~20% nuclear FOXO3 occurred when

cotransfected with T387E or K59R. T183A evidently triggered FOXO3 phosphorylation, it also strongly provoked FOXO3 nuclear translocation upon H₂O₂ stimulation (Fig. 5, A and B). The quantitative analysis is summarized in Fig. 5C. Thus, these data demonstrate that Akt phosphorylation of MstI prevents FOXO3 nuclear translocation. Inhibition of MstI phosphorylation by Akt enhances FOXO3 nuclear residency.

To further test the notion the blockage of MstI phosphorylation by Akt elicits FOXO3 nuclear residency, we transfected HEK293 cells with FOXO3, and infected the transfected cells with control adenovirus or virus expressing shRNA-Akt, followed by H₂O₂ stimulation. We monitored FOXO3 nuclear translocation by immunostaining. In the absence of H₂O₂, 11% of FOXO3 is in the control nucleus. Depletion of Akt enhanced the ratios to 38%. H₂O₂ stimulation triggered 79% FOXO3 nuclear translocation, which was further elevated to 98% when Akt was knocked down (Fig. 5D), underscoring that inhibition of MstI phosphorylation by depletion of Akt increased FOXO3 nuclear retention. These results are consistent with the observations in MstI T387A transfected cells. As an alternative approach to explore the effect of MstI phosphorylation by Akt on FOXO3 nuclear translocation, we conducted subcellular fractionation assay with various GST-MstI constructs transfected HEK293 cells. In the nuclear fraction, p-FOXO3 was markedly increased upon H₂O₂ treatment in most of GST-MstI construct-transfected cells except MstI T387E (Fig. 5E, *top panel*), an effect correlating with the quantitative nuclear translocation results. The minor ratio discrepancy between wild-type and T183A MstI in nuclear fractionation and microscopic examination might be due to the variation from the different analytical approaches. The purity of nuclear fraction was verified by immunoblotting with anti-tubulin and anti-PARP antibodies, respectively (Fig. 5E, *middle and bottom panels*). Thus, Akt phosphorylates MstI and inhibits its kinase activity on FOXO3, preventing FOXO3 nuclear translocation.

DISCUSSION

In this study, we have demonstrated that MstI acts as a physiological substrate of Akt. Akt phosphorylation of MstI protects MstI from apoptotic cleavage. Interestingly, this phosphorylation substantially enhances its *in vitro* kinase activity to H2B and completely abolishes its kinase activity to FOXO3. Moreover, we provide compelling evidence that Akt mediates MstI kinase activity on FOXO3 Ser²⁰⁷ but not on H2BS14 in intact cells. Thus, these data support that MstI possesses distinct effects on FOXO3 and histone H2B, although both nuclear proteins are implicated in apoptosis. David Allis and co-workers (16) show that MstI can phosphorylate H2B at Ser¹⁴ *in vitro* and *in vivo*, and the onset of H2BS14 phosphorylation is dependent upon cleavage of MstI by caspase-3. Moreover, H2BS14 phosphorylation correlates with apoptotic chromatin condensation, indicating that MstI phosphorylates H2BS14 and promotes apoptotic chromatin condensation. Surprisingly, MstI T387E, an Akt phosphorylation mimetic mutant, exhibits the strongest kinase activity on H2B, a nonspecific universal substrate for *in vitro* kinase assay. However, T387A fails to phosphorylate H2B, acting exactly as kinase-dead K59R *in vitro* and in transfected cells (Fig. 4, A and D). This observation suggests that MstI

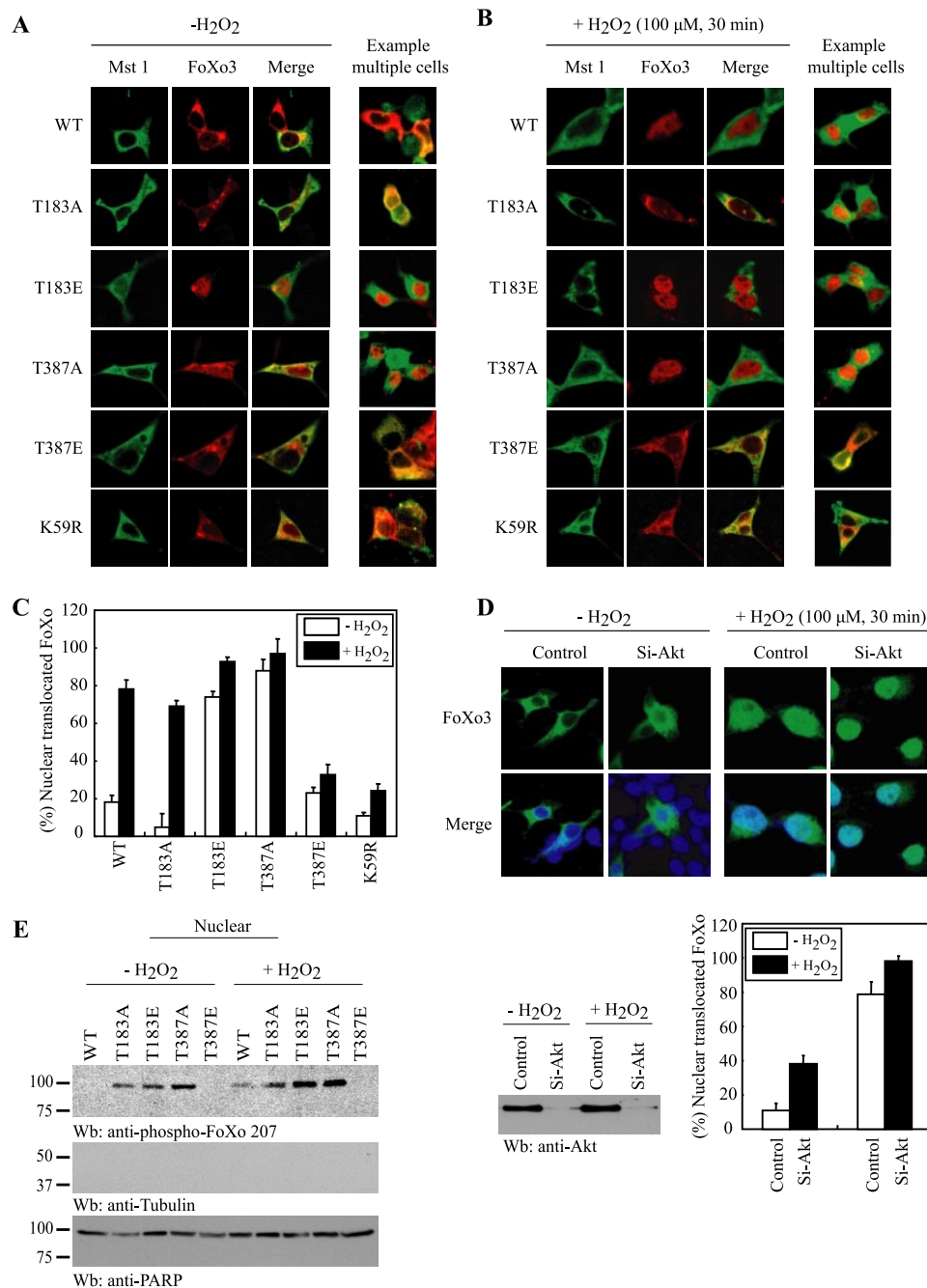


FIGURE 5. Akt phosphorylation mimetic Mstl T387E prevents H₂O₂-triggered FOXO3 nuclear translocation. A and B, T387A triggers FOXO3 nuclear translocation, whereas T387E prevents FOXO3 nuclear distribution. HEK293 cells were cotransfected with Myc-FOXO3 and various GST-Mstl constructs. The transfected cells were treated with or without H₂O₂. The transfected cells were stained with anti-Myc and anti-GST antibodies, followed by FITC- or Texas red-conjugated secondary antibodies, respectively. T183E triggered FOXO3 nuclear translocation even in the absence of H₂O₂ stimulation, which was blocked in T183A cells. Interestingly, T387A also elicited FOXO3 nuclear retention. H₂O₂ treatment provoked FOXO3 nuclear distribution in wild-type Mstl, T183A, T183E, T387A cells, but most of it remained in the cytoplasm in T387E and K59R-transfected cells. C, quantification of FOXO3 nuclear translocation in Mstl-transfected cells. Values are means (±S.D.) of three independent experiments. D, depletion of Akt enhances FOXO3 nuclear translocation. HEK293 cells were transfected with GFP-FOXO3 and endogenous Akt was knocked down with siRNA, followed by H₂O₂ treatment for 30 min. Immunofluorescent staining of transfected cells treated with or without H₂O₂ treatment (upper panels). Confirmation of Akt ablation by immunoblotting (lower left panel). Quantification of nuclear translocated GFP-FOXO3 cells (lower right panel). E, subcellular fractionation of transfected cells. The nuclear fractions were prepared from HEK293 cells, transfected with a variety of GST-Mstl constructs. H₂O₂ treatment markedly enhanced Ser²⁰⁷ phosphorylation in FOXO3 in most of Mstl construct-transfected cells except Mstl T387E (top panel). Verification of nuclear fraction purity by immunoblotting with anti-tubulin and anti-PARP (middle and bottom panels).

Thr³⁸⁷ phosphorylation by Akt is necessary for the phosphorylation of H2BS14. If H2B is a physiological substrate of MstI as claimed by Allis group, then Akt phosphorylation of MstI should decrease its kinase activity on H2BS14 to repress apoptosis, which is completely opposite to our results in Fig. 4, A and D. Hence, our finding does not support the previous report that MstI is a physiological kinase for H2B. Our discovery is supported by a recent report that H2BS14 phosphorylation is almost negligible in PKC-δ-deficient B cells compared with wild-type cells and PKC-δ but not MstI might be responsible for H2BS14 phosphorylation in apoptotic cells (22). Conceivably, MstI might regulate PKC-δ kinase activity on H2BS14 phosphorylation during apoptosis. On the other hand, we observed marked FOXO3 Ser²⁰⁷ phosphorylation *in vitro* and in transfected cells by T387A but not T387E, indicating that MstI phosphorylation by Akt blocks its kinase activity on FOXO3. This finding fits perfectly with the current paradigm that Akt promotes cell survival by phosphorylating and inhibiting pro-apoptotic proteins.

Akt phosphorylates FOXO3 and elicits its cytoplasmic translocation and association with 14-3-3, preventing its transcriptional activity (2). Recently, MstI has been reported to act oppositely. Oxidative stress triggers MstI to phosphorylate FOXO3 and promotes its nuclear translocation and dissociates from 14-3-3, enhancing neuronal apoptosis (6). Here, we show that Akt physically associates with MstI and phosphorylates it and abolishes its kinase activity on FOXO3, resulting in FOXO3 cytoplasmic retention (Fig. 5). Further, we show that T387A, a nonphosphorylated MstI mutant, possesses robust kinase activity on FOXO3 and elicits its nuclear distribution even in the absence of oxidative stress. Both gain-of-function and loss-of-function experiments support that Akt mediates FOXO3 nuclear export not only through

direct modification of FOXO3 by Akt but also through phosphorylation of MstI to block its stimulatory effect on FOXO3 nuclear translocation. Accumulative evidence supports that Akt suppresses apoptosis through phosphorylating and inhibiting pro-apoptotic effectors including Bad (23, 24), caspase-9 (25), and acinus (26) etc. Here, we provide more evidence that Akt promotes cell survival by phosphorylating and inhibiting the apoptotic kinase MstI.

MstI acting as an apoptotic kinase requires both caspase cleavage and phosphorylation (11, 27). Interestingly, MstI may function both upstream and downstream of caspases, because exogenously expressed MstI activates caspases, which results in its own cleavage (13). In the current study, we show that Akt phosphorylates MstI and protects it from apoptotic process (Fig. 3). Although Akt directly binds MstI, which might shield MstI from proteolytic attack; however, we show that T387E, a phosphorylation mimetic mutant, resists against caspase-mediated cleavage, whereas T387A, a nonphosphorylated mutant, displays the fastest degradation effect. These results support that Akt protects MstI through phosphorylation on Thr³⁸⁷ residue. Recently, it has been report that MstI and RanBP2 levels are elevated in transgenic animals that express a constitutively active p110- α subunit in the epithelial cells of the prostate. Additionally, Akt phosphorylation, MstI and RanBP2 protein levels, can be inhibited in transgenic animals by LY294002 (28). This finding is consistent with our conclusion that Akt phosphorylation of MstI protects it from apoptotic degradation. Taken together, our findings demonstrate that MstI is a physiological substrate of Akt. In addition to direct phosphorylation of FOXOs, Akt exerts its anti-apoptotic action on FOXOs by phosphorylation of MstI and blockage of its kinase activity.

Acknowledgment—We thank Dr. Alfred Reszka at Merck Research Laboratories, West Point, PA for providing various MstI plasmids.

REFERENCES

1. Kops, G. J., and Burgering, B. M. (1999) *J. Mol. Med.* **77**, 656–665
2. Brunet, A., Bonni, A., Zigmond, M. J., Lin, M. Z., Juo, P., Hu, L. S., Anderson, M. J., Arden, K. C., Blenis, J., and Greenberg, M. E. (1999) *Cell* **96**, 857–868
3. Biggs, W. H., 3rd, Meisenhelder, J., Hunter, T., Cavenee, W. K., and Arden, K. C. (1999) *Proc. Natl. Acad. Sci. U. S. A.* **96**, 7421–7426
4. Van Der Heide, L. P., Hoekman, M. F., and Smidt, M. P. (2004) *Biochem. J.* **380**, 297–309
5. Brownawell, A. M., Kops, G. J., Macara, I. G., and Burgering, B. M. (2001) *Mol. Cell Biol.* **21**, 3534–3546
6. Lehtinen, M. K., Yuan, Z., Boag, P. R., Yang, Y., Villen, J., Becker, E. B., DiBacco, S., de la Iglesia, N., Gygi, S., Blackwell, T. K., and Bonni, A. (2006) *Cell* **125**, 987–1001
7. Creasy, C. L., and Chernoff, J. (1995) *J. Biol. Chem.* **270**, 21695–21700
8. Creasy, C. L., Ambrose, D. M., and Chernoff, J. (1996) *J. Biol. Chem.* **271**, 21049–21053
9. Graves, J. D., Draves, K. E., Gotoh, Y., Krebs, E. G., and Clark, E. A. (2001) *J. Biol. Chem.* **276**, 14909–14915
10. Lee, K. K., Ohshima, T., Yajima, N., Tsubuki, S., and Yonehara, S. (2001) *J. Biol. Chem.* **276**, 19276–19285
11. Glantschnig, H., Rodan, G. A., and Reszka, A. A. (2002) *J. Biol. Chem.* **277**, 42987–42996
12. Lee, K. K., Murakawa, M., Nishida, E., Tsubuki, S., Kawashima, S., Sakamaki, K., and Yonehara, S. (1998) *Oncogene* **16**, 3029–3037
13. Graves, J. D., Gotoh, Y., Draves, K. E., Ambrose, D., Han, D. K., Wright, M., Chernoff, J., Clark, E. A., and Krebs, E. G. (1998) *EMBO J.* **17**, 2224–2234
14. Lin, Y., Khokhlatchev, A., Figeys, D., and Avruch, J. (2002) *J. Biol. Chem.* **277**, 47991–48001
15. Ura, S., Masuyama, N., Graves, J. D., and Gotoh, Y. (2001) *Proc. Natl. Acad. Sci. U. S. A.* **98**, 10148–10153
16. Cheung, W. L., Ajiro, K., Samejima, K., Kloc, M., Cheung, P., Mizzen, C. A., Beeser, A., Etkin, L. D., Chernoff, J., Earnshaw, W. C., and Allis, C. D. (2003) *Cell* **113**, 507–517
17. Praskova, M., Khokhlatchev, A., Ortiz-Vega, S., and Avruch, J. (2004) *Biochem. J.* **381**, 453–462
18. Oh, H. J., Lee, K. K., Song, S. J., Jin, M. S., Song, M. S., Lee, J. H., Im, C. R., Lee, J. O., Yonehara, S., and Lim, D. S. (2006) *Cancer Res.* **66**, 2562–2569
19. Liu, X., Kim, C. N., Yang, J., Jemmerson, R., and Wang, X. (1996) *Cell* **86**, 147–157
20. Ye, K., Ke, Y., Keshava, N., Shanks, J., Kapp, J. A., Tekmal, R. R., Petros, J., and Joshi, H. C. (1998) *Proc. Natl. Acad. Sci. U. S. A.* **95**, 1601–1606
21. Brazil, D. P., Park, J., and Hemmings, B. A. (2002) *Cell* **111**, 293–303
22. Blois, J. T., Mataraza, J. M., Mecklenbrauker, I., Tarakhovsky, A., and Chiles, T. C. (2004) *J. Biol. Chem.* **279**, 30123–30132
23. Datta, S. R., Dudek, H., Tao, X., Masters, S., Fu, H., Gotoh, Y., and Greenberg, M. E. (1997) *Cell* **91**, 231–241
24. del Peso, L., Gonzalez-Garcia, M., Page, C., Herrera, R., and Nunez, G. (1997) *Science* **278**, 687–689
25. Cardone, M. H., Roy, N., Stennicke, H. R., Salvesen, G. S., Franke, T. F., Stanbridge, E., Frisch, S., and Reed, J. C. (1998) *Science* **282**, 1318–1321
26. Hu, Y., Yao, J., Liu, Z., Liu, X., Fu, H., and Ye, K. (2005) *EMBO J.* **24**, 3543–3554
27. de Souza, P. M., and Lindsay, M. A. (2004) *Biochem. Soc. Trans.* **32**, 485–488
28. Renner, O., Fominaya, J., Alonso, S., Blanco-Aparicio, C., Leal, J. F., and Carnero, A. (2007) *Carcinogenesis*, **28**, 1418–1425